Electronic Supplementary Material (ESI) for Dalton Transactions
This journal is © The Royal Society of Chemistry 2013

SUPPORTING INFORMATION

Kinetics and mechanism of oxidation of super-reduced cobalamin and cobinamide species by thiosulfate, sulfite and dithionite

Ilia A. Dereven'kov, Denis S. Salnikov, Sergei V. Makarov, Gerry R. Boss and Oskar I. Koifman

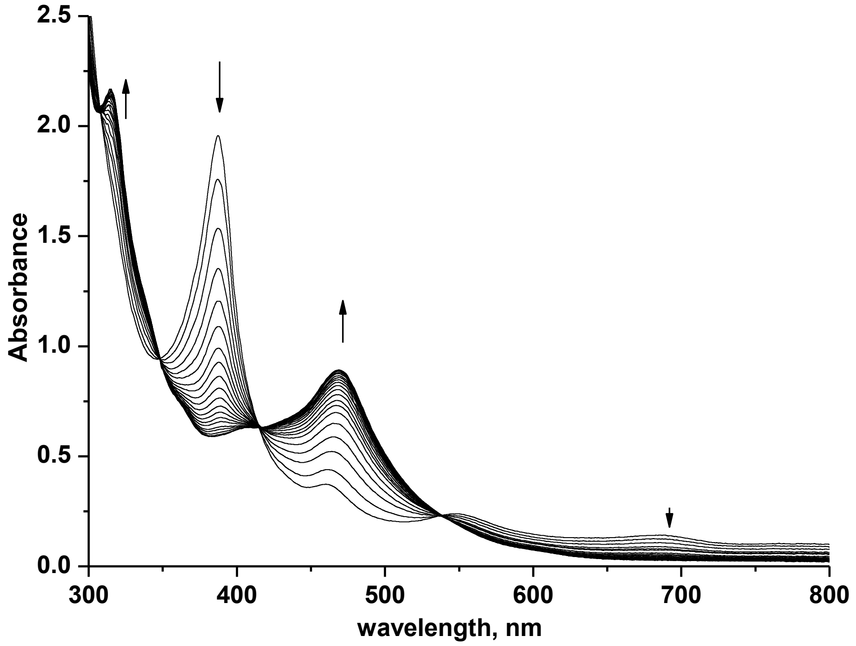

Fig. S1. UV-Vis spectral changes collected during the oxidation of Cbi(I) by thiosulfate. [Cbi] = 7×10^{-5} M; [$S_2O_3^{2-}$] = 1×10^{-3} M; pH 9.4; 25°C.

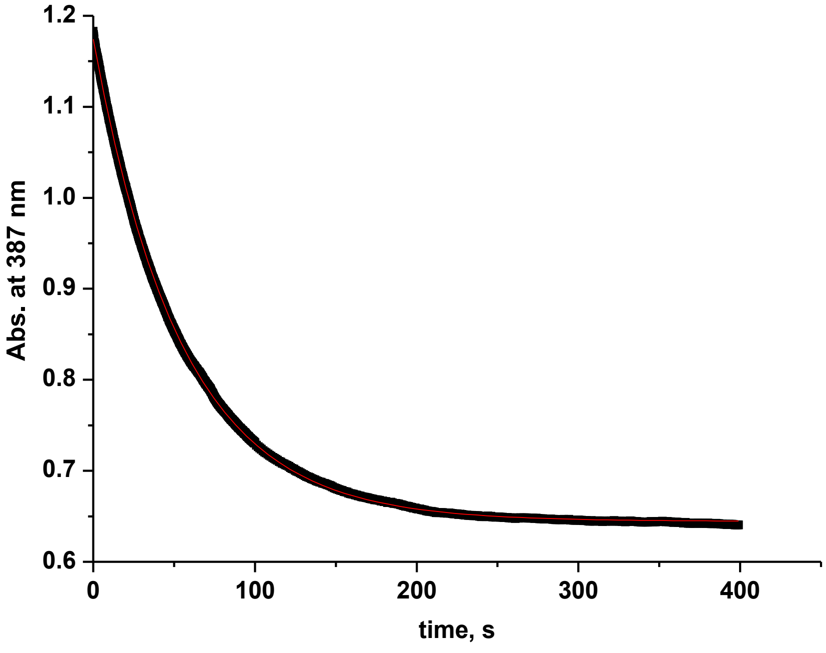

Fig. S2. Example of kinetic curve of the oxidation of Cbi(I) (6×10^{-5} M) by thiosulfate (2×10^{-3} M) at pH 9.4; 25°C.

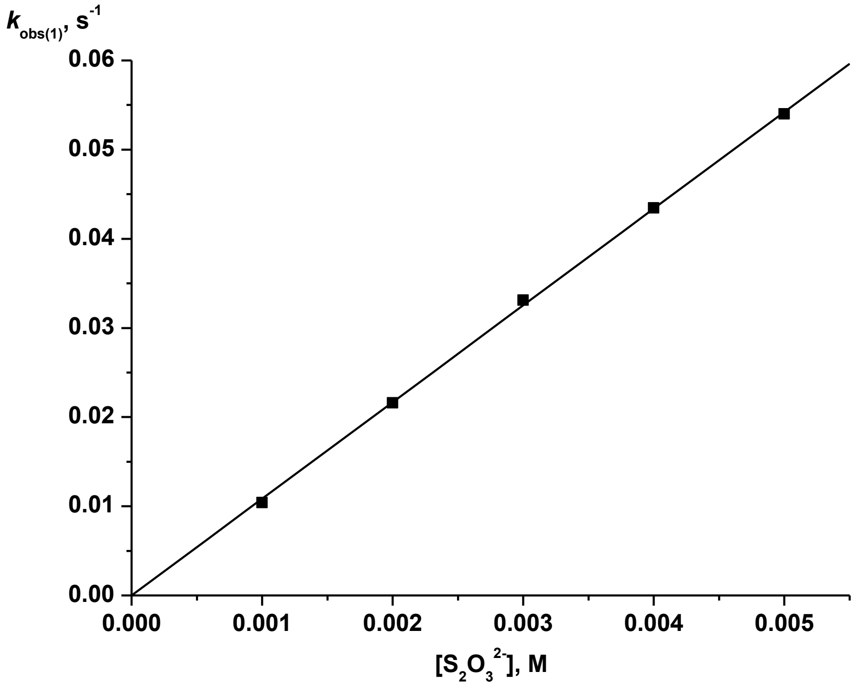

Fig. S3. Dependence of $k_{obs(1)}$ on $[S_2O_3^{2-}]$ for the reaction between Cbi(I) (6×10^{-5} M) and thiosulfate at pH 9.08; 25°C.

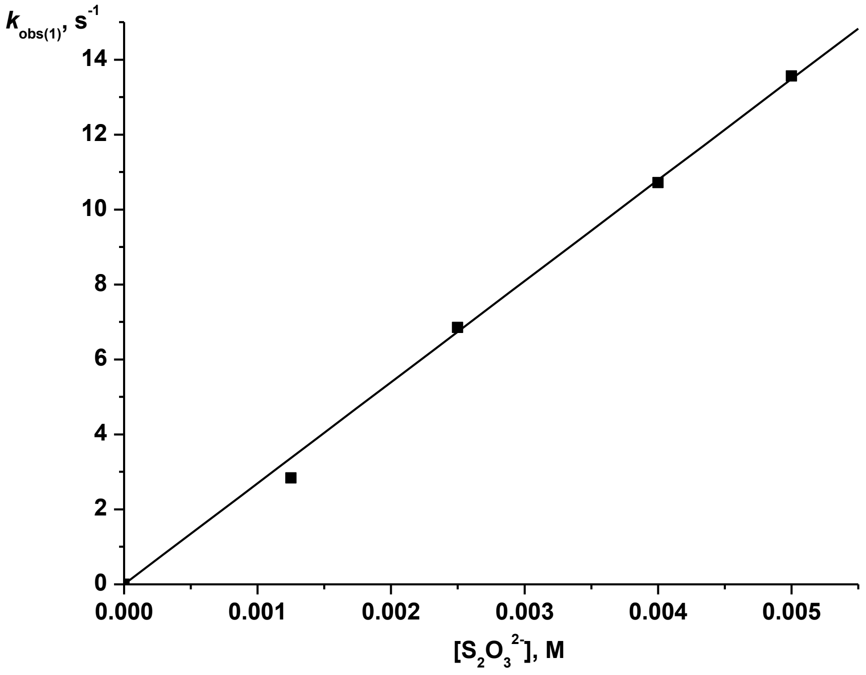

Fig. S4. Plot of $k_{obs(1)}$ *vs*. $[S_2O_3^{2-}]$ for the oxidation of Cbl(I) (5×10^{-5} M) by thiosulfate at pH 5.9; 25°C.

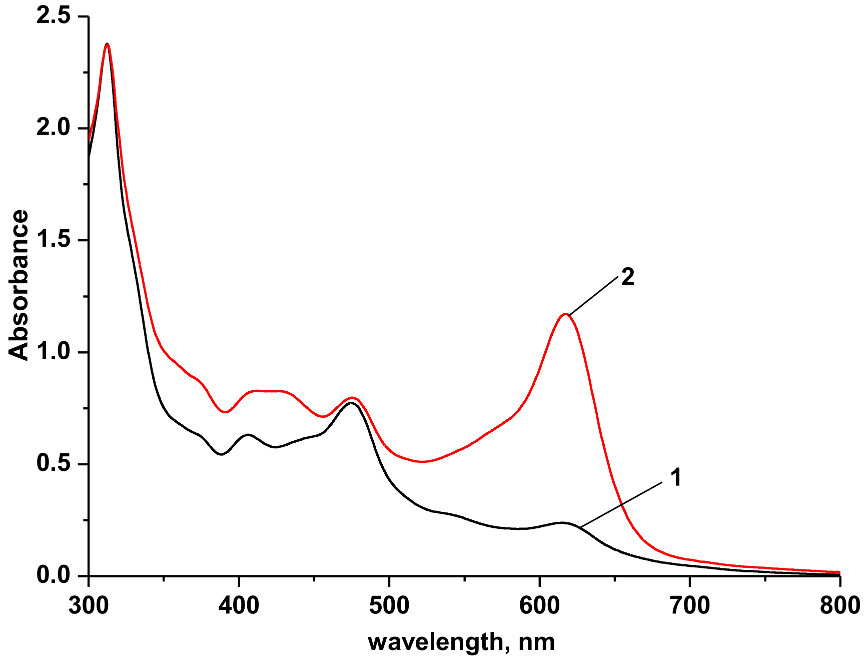

Fig. S5. UV-Vis spectra recorded after the addition of malachite green (8.8×10^{-6} M) to the mixture immediately after the reaction Cbl(I) + $S_2O_3^{2-}$ (1) and to the mixture Cbl(II) + $S_2O_3^{2-}$ (control experiment) (2). [Cbl] = 6×10^{-5} M; [$S_2O_3^{2-}$] = 6×10^{-4} M; pH 7.2; 25°C.

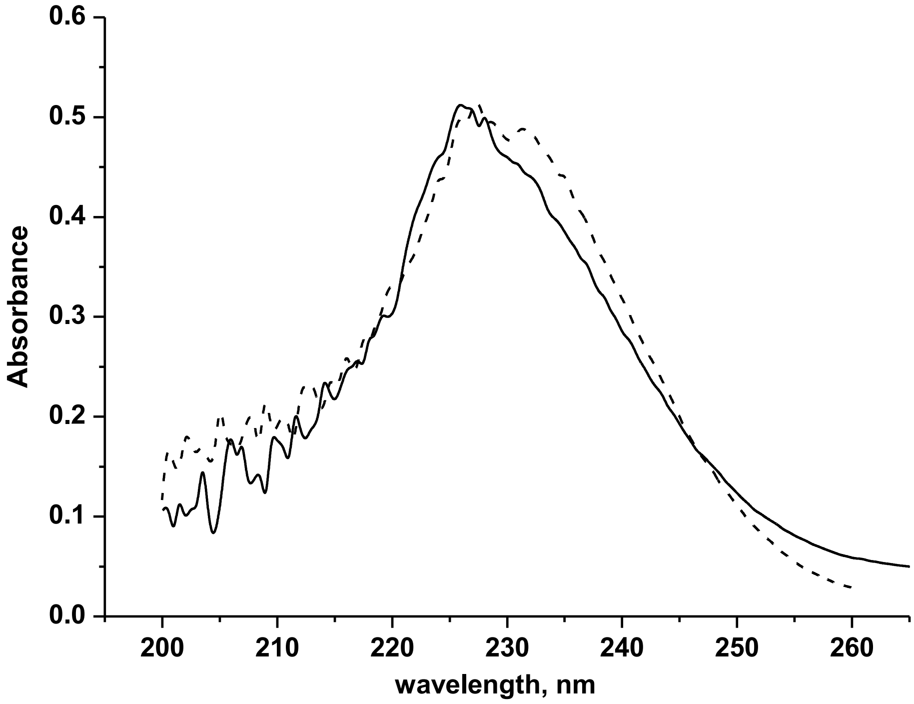

Fig. S6. UV spectra of 0.1 M Na_2CO_3 containing dissolved volatile components of reaction mixture (solid line) and 7×10^{-5} M HS^- (dashed line). Reaction mixture (3 ml.) in the first case contained 1×10^{-4} M $Na_2S_2O_3$ and 5×10^{-4} M Cbl(I) at pH 7. After the completion of the reaction the mixture was acidified by H_3PO_4 to pH 3, then slow argon stream was bubbled for two hours subsequently through reaction mixture and deoxygenated Na_2CO_3 (3 ml.).

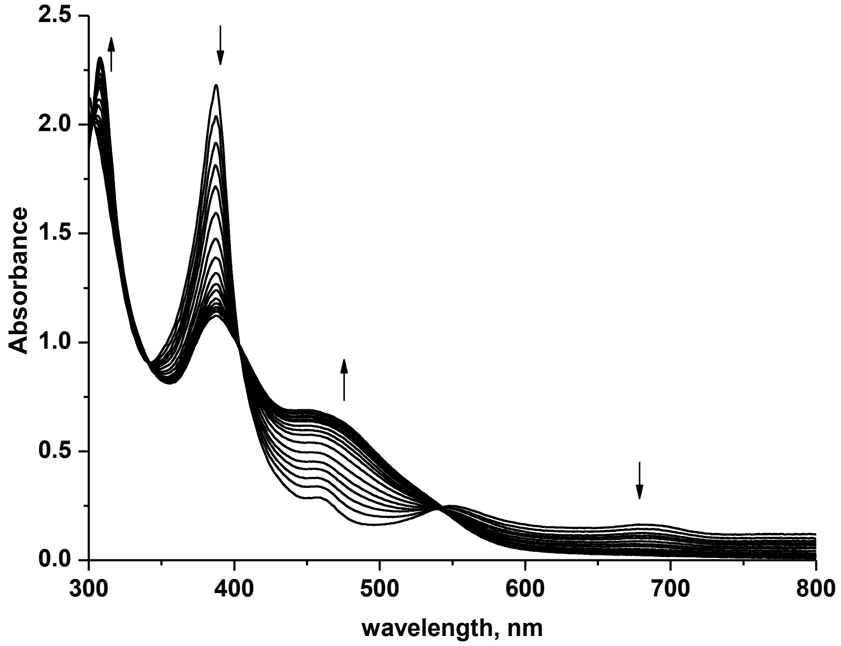

Fig. S7. UV-Vis spectral changes recorded in the course of the oxidation of Cbi(I) by sulfite. [Cbi] = 8×10^{-5} M; [SO_3^{2-}] = 1×10^{-2} M; pH 9.4; 25°C.

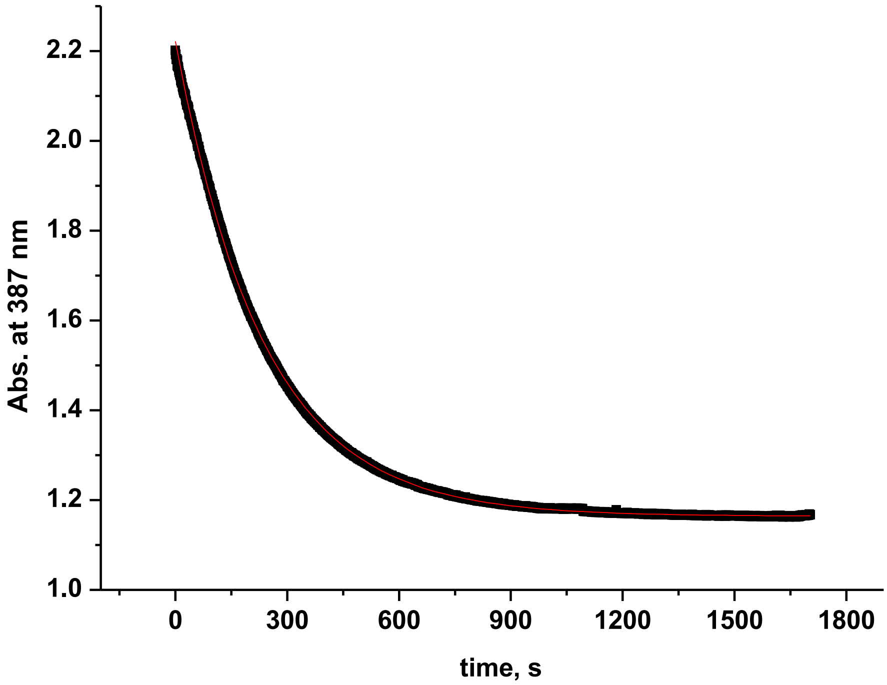

Fig. S8. Typical kinetic curve of the oxidation of Cbi(I) (8×10^{-5} M) by sulfite (2×10^{-2} M) at pH 9.8; 25°C.

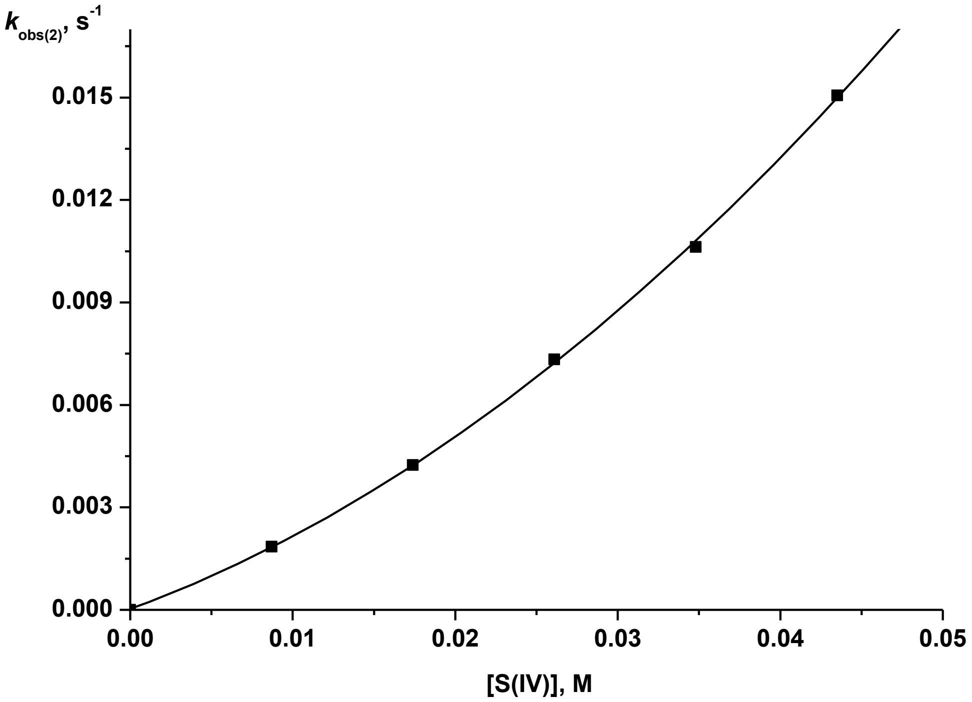

Fig. S9. Plot of $k_{obs(2)}$ *vs*. [S(IV)] for the reaction between Cbi(I) (5×10^{-5} M) and sulfite at pH 9.7; 25°C.

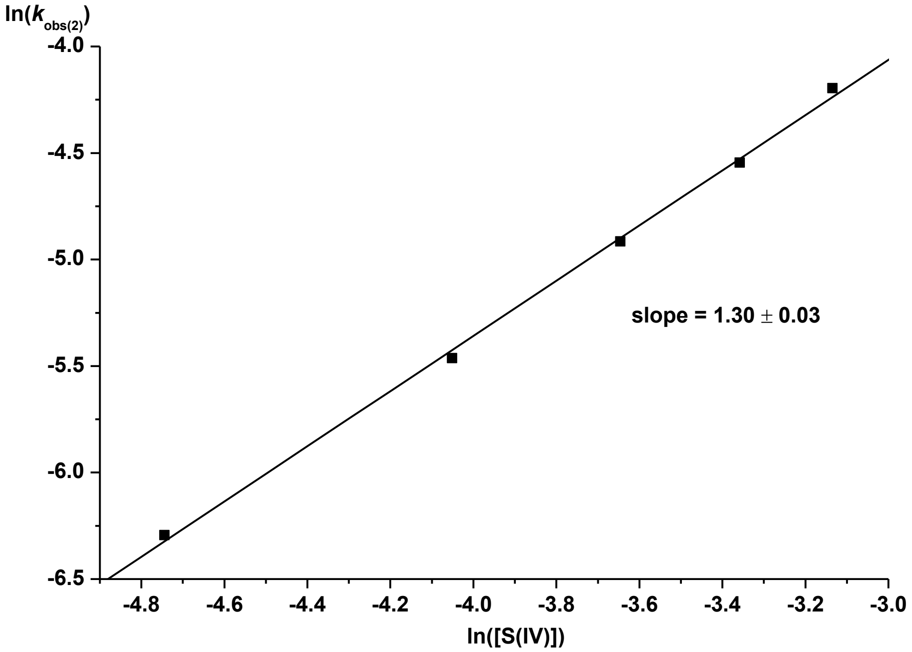

Fig. S10. Plot of ln($k_{obs(2)}$) *vs*. ln([S(IV)]) for the reaction between Cbi(I) (5×10^{-5} M) and sulfite at pH 9.7; 25°C.

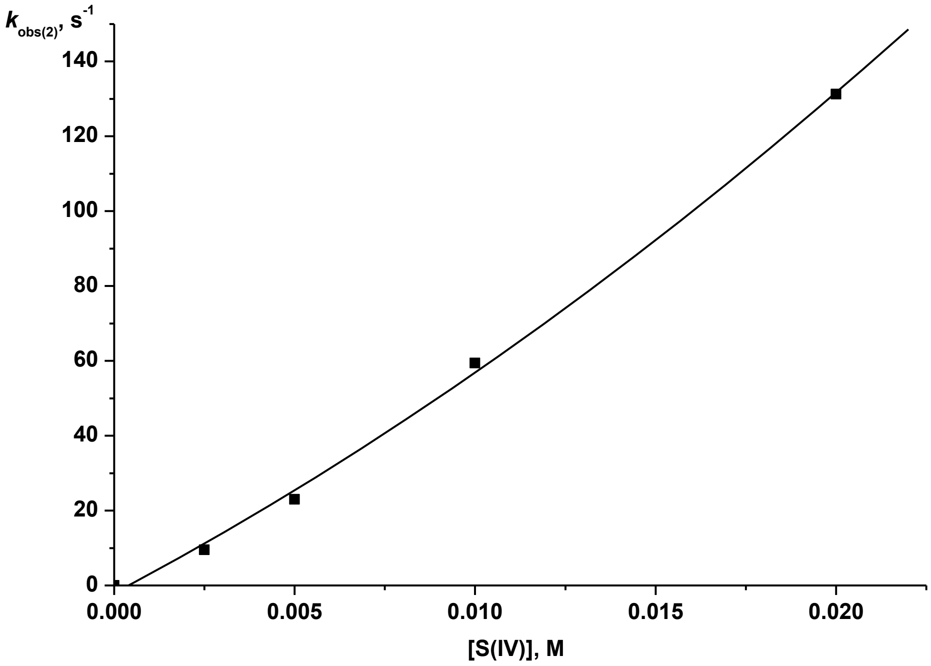

Fig. S11. Plot of $k_{obs(2)}$ vs. [S(IV)] for the reaction of Cbl(I) (5×10^{-5} M) with sulfite at pH 6.4; 25°C.

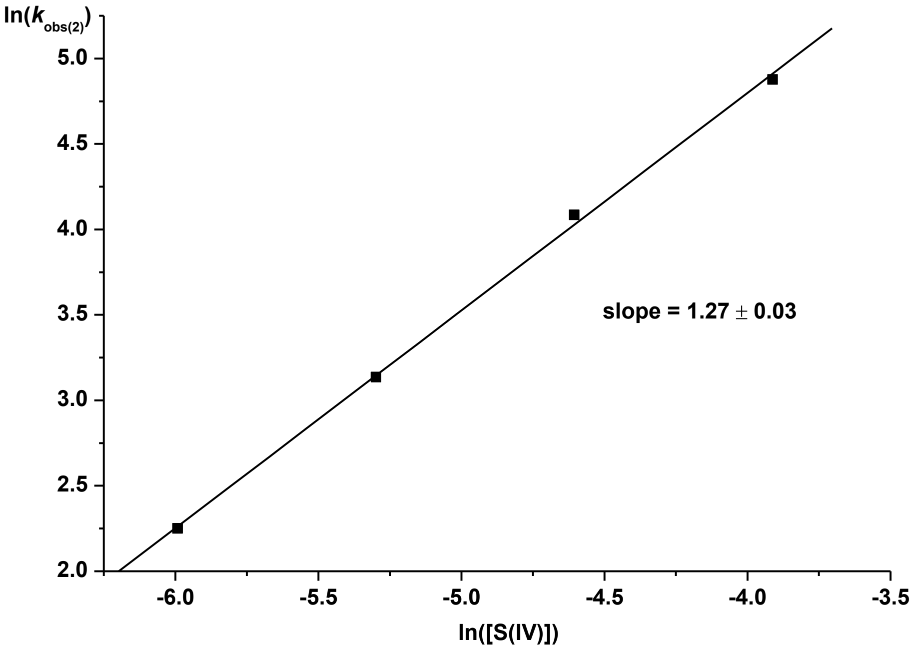

Fig. S12. Plot of ln($k_{obs(2)}$) *vs*. ln([S(IV)]) for the reaction between Cbl(I) (5×10^{-5} M) and excess sulfite at pH 6.4; 25°C.

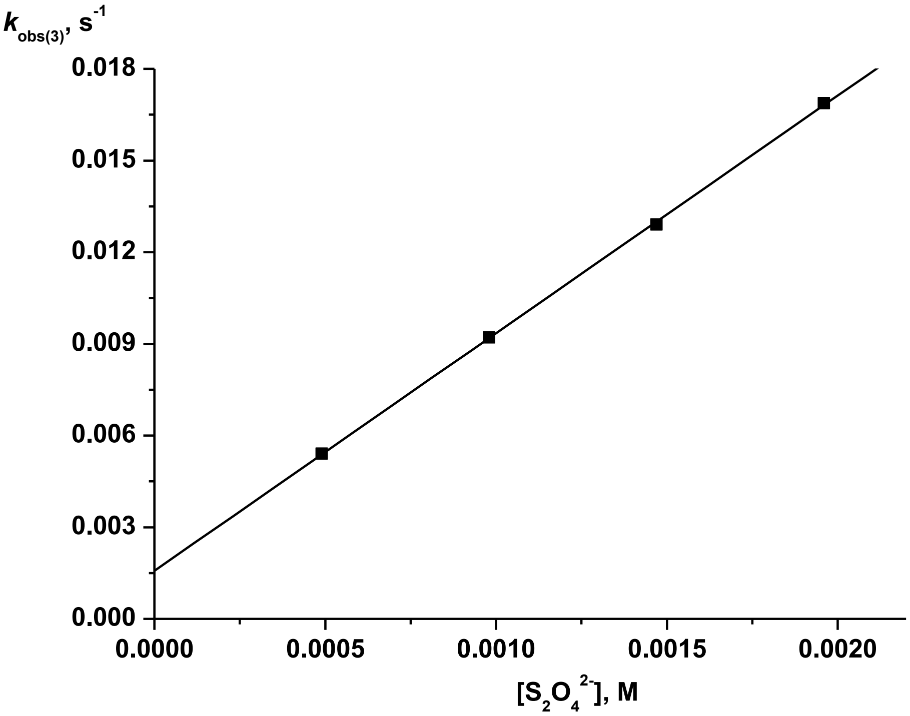

Fig. S13. Plot of $k_{obs(3)}$ *vs*. [$S_2O_4^{2-}$] for the oxidation of Cbi(I) (7×10^{-5} M) by dithionite at pH 10; 25°C.

Kinetics of cob(II)inamide reduction by sulfoxylate in aqueous solutions

Experimental. Cobinamide was prepared and purified according to reported procedure [S1]. Hydroxocobalamin hyrochloride (HOCbl, ≥98 %), thiourea dioxide (TDO), ascorbic acid (AA), sodium dithionite (85 %) were purchased in Sigma-Aldrich and used as received. Other chemical were of a reagent grade. Triple distilled water was used to the preparation of solutions. Oxygen-free argon was used to deoxygenate solutions.

Kinetic measurements were performed on a thermostated (± 0.1°C) Cary 50 spectrophotometer in anoxic conditions in sealed quartz cells. The constant values of pH were maintained by NaOH, H_3BO_3, Na_2CO_3 solutions.

Sulfoxylate solutions SO_2H^- (SO_2^{2-}) were prepared during "aging" TDO in anaerobic 0.1 M NaOH for 4 hours [S2]. Urea formed during the decomposition of TDO does not influence on the rate of reactions [S3].

Kinetics of the formation of Co(I) cobinamide was monitored at 387 nm (the maximum of absorbance of Cbi(I)). In the presence of dithionite kinetics was studied at 460 nm.

Results. The discussion of reported below data is similar to that in [S4]. UV-Vis spectra of initial complexes and products are in Fig. S14. Further, is considered. Reactions orders for the step of the formation of Cbi(I) in both cobinamide and sulfoxylate were found to be the first. The rate constant of the reduction of Cbi(II)–SO_2^- by sulfoxylate is 2.18 ± 0.07 M^{-1} s^{-1} (Fig. S15). The rate constant of the reduction of Cbi(II) (preliminarily produced from Cbi(III) by AA use) by sulfoxyalte is 3.30 ± 0.11 M^{-1} s^{-1}. The dependence of observed rate constant of the Cbi(II)–SO_2^- reduction by sulfoxylate on pH exhibits a profile corresponding to S-shaped curve (Fig. S15). Its fitting to sigmoidal curve equation gives $pK_a = 13.47 \pm 0.07$.

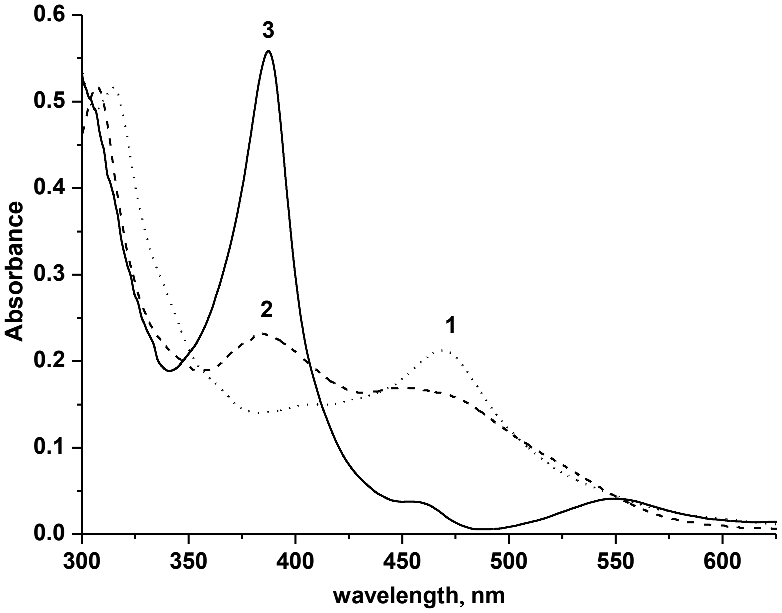

Fig. S14. UV-Vis spectra of Cbi species: 1 – Cbi(II) obtained using AA; 2 - Cbi(II)–SO_2^-; 3 – Cbi(I). [Cbi] = 2×10^{-5} M; [AA] = 4×10^{-4} M; [SO_2^{2-}] = 1×10^{-3} M; pH 13; 25 °C.

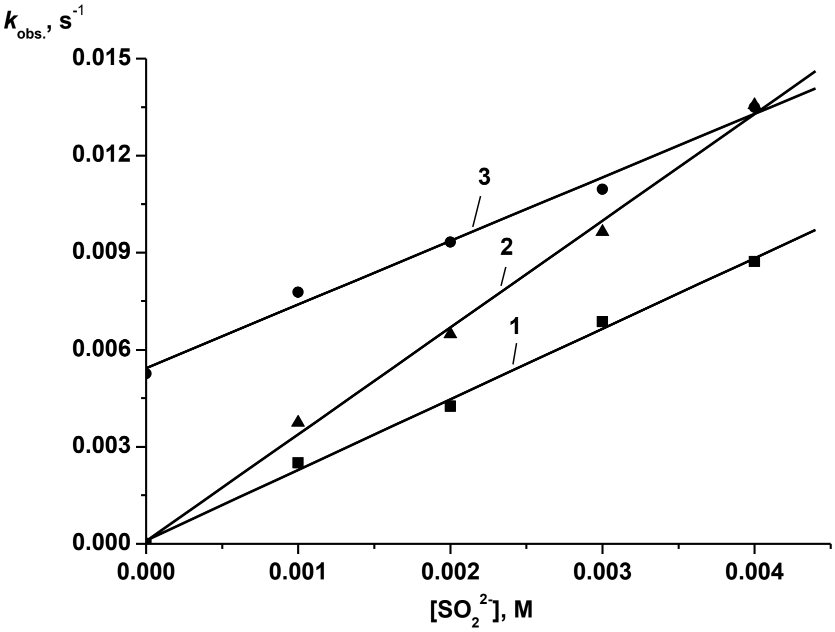

Fig. S15. Plot of $k_{obs.}$ *vs*. [SO_2^{2-}] for reactions of Cbi(I) accumulation during the reduction of Cbi(II)(SO_2^-) (1), Cbi(II) (2) and Cbi(II)(SO_2^-) in the presence of 3.3 mM $S_2O_4^{2-}$ (3) by sulfoxylate. [Cbi] = 2×10^{-5} M; pH 13; 25 °C.

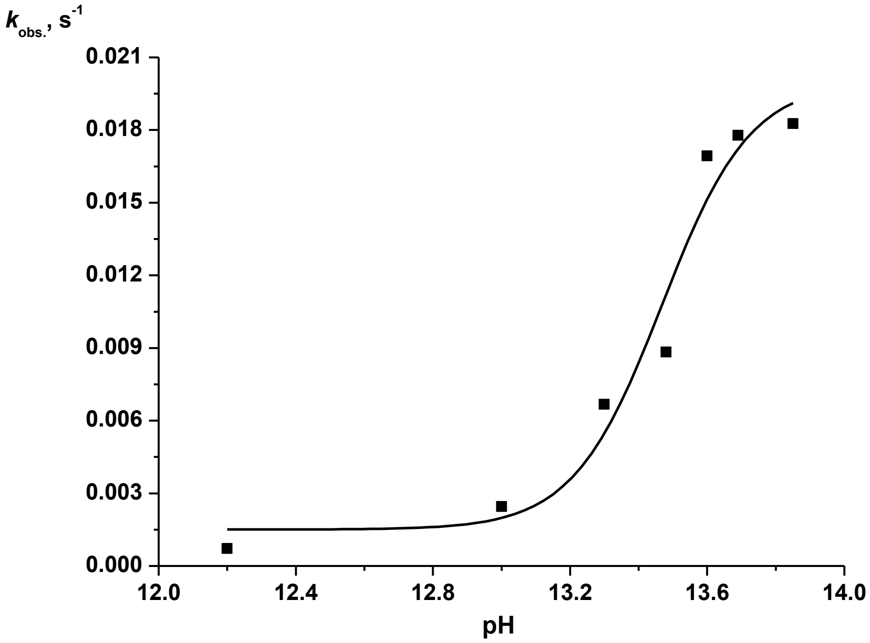

Fig. S16. Plot of observed rate constant of Cbi(I) formation *vs*. pH. [Cbi] = 2×10^{-5} M; [SO_2^{2-}] = 1×10^{-3} M; 25 °C.

References

S1) W. C. Blackledge, C. W. Blackledge, A. Griesel, S. B. Mahon, M. Brenner, R. B. Pilz, G. R. Boss, *Anal Chem*, 2010, **82**, 4216–4221.

S2) S.V. Makarov, E. V. Kudrik, R. van Eldik, E.V. Naidenko, *J. Chem. Soc., Dalton Trans.*, 2002, 4074–4076.

S3) S. A. Svarovsky, R. H. Simoyi, S. V. Makarov, *J. Chem. Soc., Dalton Trans.*, 2000, 511–514.

S4) D. S. Salnikov, I. A. Dereven'kov, S. V. Makarov, E. S. Ageeva, A. Lupan, M. Surducan, R. Silaghi-Dumitrescu, *Rev. Roum. Chim.*, 2012, **57**, 353–359.